DISCRETE AND CONTINUOUS
DYNAMICAL SYSTEMS SERIES B
Volume **12**, Number **2**, September **2009**

doi:10.3934/dcdsb.2009.12.371

pp. **371–388**

A DEGENERATE DIFFUSION-REACTION MODEL OF AN AMENSALISTIC BIOFILM CONTROL SYSTEM: EXISTENCE AND SIMULATION OF SOLUTIONS

Hassan Khassehkhan

Department of Mathematics and Statistics
University of Guelph, Guelph, On, N1G 2W1, Canada

Messoud A. Efendiev

Institute of Biomathematics and Biometry, HelmholtzZentrum München
Ingolstädter Landstrasse 1, 85764 Neuherberg, Germany

Hermann J. Eberl

Department of Mathematics and Statistics
University of Guelph, Guelph, On, N1G 2W1, Canada

Abstract. We study a mathematical model that describes how a "good" bacterial biofilm controls the growth of a harmful pathogenic bacterial biofilm. The underlying mechanism is a modification of the local protonated acid concentration, which in turn decreases the local pH and, thus, makes growth conditions for the pathogens less favorable, while the control-agent itself is more tolerant to these changes. This system is described by a system of 5 density-dependent diffusion-reaction equations that show two nonlinear diffusion effects: porous medium degeneracy and fast diffusion. This is a multi-species expansion of a previously studied single species biofilm model. In this paper we prove the existence of solutions to this model and show in numerical simulations the effectiveness of the control mechanism.

1. **Introduction.** Biofilms are microbial depositions on immersed surfaces [19]. If the environmental conditions are such that they can sustain bacterial life, cells attach to the surface (also called substratum in the biofilm context) and start the production of extracellular polymeric substances (the so-called EPS). The cells themselves are embedded in this layer. This offers them protection against harmful environmental impacts, such as mechanical wash-out or antimicrobials, which meet stronger diffusive resistance in the EPS matrix than in the liquid phase. Moreover, since many antibiotics are neutralized upon contact with cells, they often are only able to inactivate the cells closest to the biofilm/liquid interface, while the cells in the deeper regions of the biofilm, close to the substratum, remain virtually unharmed. This makes traditional antibiotic control of biofilms much more cumbersome than the control of free-swimming, planktonic bacterial cultures. Unfortunately, however, most bacteria live in biofilms, rather than in the planktonic mode of growth, on which experimental microbiologists as well as mathematical biologist traditionally focused. This is in particular of concern in medicine, where

2000 *Mathematics Subject Classification.* Primary: 35K65; Secondary: 92D25.
Key words and phrases. nonlinear diffusion, degeneracy, biofilm, probiotic, simulation.
This study was supported in part by the Advanced Foods and Materials Network (AFMNet).

biofilms cause bacterial infections, and in food industry, where biofilm contaminations lead to hygienic and health risks. On the other hand, biofilms are beneficially used by environmental engineers who develop biofilm based technologies for tasks such as wastewater treatment, soil remediation, and groundwater protection.

Despite their name, biofilms can develop in highly complicated, spatially structured architectures, as revealed by modern microscopy techniques. Since the traditional one-dimensional biofilm models are naturally not able to capture the sometimes highly complex spatial organization, this observation made the development of multi-dimensional models necessary. The biofilm model that we are concerned with in this study is a quasilinear diffusion-reaction system that shows two nonlinear diffusion effects, porous medium degeneracy and fast diffusion. This biofilm modeling framework was originally proposed in [7] for a prototype biofilm system, and later extended to study various biofilm systems, primarily in numerical simulations [4, 6, 8, 9, 10, 11, 17]. Since the model combines two non-linear degenerating diffusion effects, standard theory does not apply in a straightforward manner. Only few rigorous analytical results are known [4, 5, 13, 14, 15], which are primarily concerned with the single species case where in particular the existence of unique solutions and of a global attractor were established.

We propose here a mathematical model in which the growth of a pathogenic bacterial population is controlled by the accumulation of protonated acids and decreasing pH. More specifically, we consider a competitive system in which microbial bio-control agents (lactic acid bacteria, LAB) modify the environmental conditions such that they become less favorable for the pathogen, while the control agents themselves are more tolerant to these self-inflicted changes in the environment. Such amensalistic microbial systems have been proposed to enhance the food safety of minimally processed refrigerated vegetable products, cf [2] and the references therein. The objective of using such live bio-control agents is not to ferment foods but to control the microbial ecology if spoilage occurs. A similar control mechanism, based on modification of pH and protonated lactic acid concentrations such that the environmental conditions become unfavorable for pathogens, is also developed by certain probiotic bacteria. These are defined as live food ingredients that confer health benefits to the host if administered in sufficient quantities [16]. Traditionally, they are used as functional foods, primarily in dairy products such as yogurt. More recently also their potential as alternative to antibiotics in medical treatments is investigated [3].

A mathematical model of this amensalistic bio-control mechanism was suggested in [2] for planktonic populations and numerically tested against experiments. In [17] this was adapted to model a pathogenic biofilm that is controlled by bio-control agents, which are suspended in the bulk but do not attach to the surface to form biofilms themselves. Now we take this one step further and adapt this to model amenalistic control of a pathogenic biofilm by a "probiotic" lactic acid producing biofilm. To this end the single-species biofilm model [17] needs to be extended into a mixed-culture setting. We will give the first existence proof for mixed-culture biofilm models of this kind and illustrate the model behavior in numerical simulations.

2. **Governing equations.**

The mathematical model of a pathogenic biofilm that is controlled by a probiotic biofilm that modifies the environmental conditions in the system is formulated in terms of the five dependent variables concentration of

protonated lactic acids, C, concentration of hydrogen ions, P, volume fraction occupied by the pathogens, N_1, volume fraction occupied by the probiotics, N_2, and volume fraction occupied by inert biomass, Y. Note that we do not distinguish between inert pathogens and inert probiotics. As is common in most biofilm modeling studies, with but few exceptions, the EPS is implicitly subsumed in the biomass fractions. The model is a multi-species generalization of the single-species probiotic biofilm control model [17]. We denote by $t \geq 0$ the independent variable time and by $x \in \Omega$, Ω a bounded domain, the independent space variable. The model reads then for $t > 0$ and $x \in \Omega$

$$\begin{aligned}
\partial_t C &= \nabla \cdot (D_C(M)\nabla C) + \alpha_1 N_1(k_1 - C) + \alpha_2 N_2(k_1 - C), && (1)\\
\partial_t P &= \nabla \cdot (D_P(M)\nabla P) + \alpha_3 C(k_2 - P), && (2)\\
\partial_t N_1 &= \nabla\cdot(D_M(M)\nabla N_1) + \mu_1 g_1(C,P)N_1, && (3)\\
\partial_t N_2 &= \nabla\cdot(D_M(M)\nabla N_2) + \mu_2 g_2(C,P)N_2, && (4)\\
\partial_t Y &= \nabla\cdot(D_M(M)\nabla Y) - \min(0,\mu_1 g_1(C,P)N_1) - \min(0,\mu_2 g_2(C,P)N_2), && (5)
\end{aligned}$$

where the ∇ operator is taken with respect to x. All constant parameters in (1)-(5) are non-negative. The density dependent biomass diffusion coefficient is

$$D_M(M) = d\frac{M^a}{(1-M)^b}, \quad M = N_1 + N_2 + Y \tag{6}$$

where $a, b > 1$ and the biomass motility coefficient d is a very small positive number [7]. It is several orders of magnitudes smaller than the diffusion coefficients $D_{C,P}$ of the dissolved substrates. The variable $M(t,x)$ denotes the volume fraction occupied by biomass of either particulate substance, active or inert biomass. This controls the spatial spreading of biomass. The power law M^a guarantees that biomass does not spread if the local density is small; the power law $(1-M)^{-b}$ guarantees that the biomass density remains bounded by the maximum possible cell density, even if inside the biofilm production of new biomass continues. Thus, the model includes both, finite speed of interface propagation (between biofilm and aqueous phase) and volume filling features. The actual biofilm is thus the region $\Omega_2(t) := \{x \in \Omega : M(t,x) > 0\}$. The region $\Omega_1(t) := \{x \in \Omega : M(t,x) \equiv 0\}$ is the surrounding liquid phase. The biofilm liquid interface is $\Gamma(t) := \bar{\Omega}_1(t) \cap \bar{\Omega}_2(t)$. In this model we assume implicitly that spatial movement of both biomass fractions, probiotic and pathogen, is described by exactly the same spatial operator. Strictly speaking this need not be the case, but would depend on the particular microbial species involved. This assumption is made here for simplicity and in the absence of additional information that would warrant a more complicated *ansatz*.

In [23] it is pointed out that the role that diffusion of dissolved substrates plays, in our case C and P, constitutes the main difference between biofilm communities and suspended cultures. While in the latter case all cells experience the same conditions, in biofilm communities often dissolved substrates cannot completely penetrate the biofilm or only at a reduced concentration. Moreover, the biofilm poses an increased resistance to diffusing substrates. Therefore, we assume $D_{C,P}$ to be dependent on the density of the biofilm matrix, M as well. We make a linearization *ansatz*,

$$D_{C,P}(M) = D_{C,P}(0) - M(D_{C,P}(0) - D_{C,P}(1)) \tag{7}$$

where $D_{C,P}(0)$ is the diffusion coefficient in water and $D_{C,P}(1)$ is the diffusion coefficient in a fully developed biofilm. Thus $D_{C,P}(M)$ are bounded from below

and above by known positive constants. Since inside the biofilm $M \approx 1$, diffusion in both the aqueous and the biofilm phase behaves essentially like Fickian diffusion.

The reaction terms on the right hand side of (1)-(5) stem from [2], based on previous work of [21]. They have the following meaning:

Protonated acids, C. Protonated lactic acids are produced by both bacterial species until locally a maximum concentration is reached.

Hydrogen ion concentration, P. The local hydrogen ion concentration increases (pH decreases) until a saturation level is reached. This is facilitated by the lactic acids. The concentration P and the local pH value are related by

$$\text{ph} = -\log P$$

if P is measured in moles.

Biomass fractions, N_1, N_2, Y. Biomass production is controlled by C and P. The growth/inhibition functions $g_{1,2}(C,P)$ in the equations for N_1, N_2, Y are piecewise linear, such that they are positive if both C and P are small, and become negative if one of C and P becomes large. Between the growth and inhibition range there is an extended neutral range. More specifically,

$$g_i(C,P) = \min\left\{1 - \frac{C}{H_1^{(i)}(C)}, 1 - \frac{P}{H_2^{(i)}(P)}\right\}, \tag{8}$$

where the auxiliary functions $H_1^{(i)}(C)$ and $H_2^{(i)}(P)$ are defined by

$$H_1^{(i)}(C) = k_1^{(i)} H(k_1^{(i)} - C) + C \cdot H(C - k_1^{(i)}) \cdot H(k_2^{(i)} - C) + k_2^{(i)} H(C - k_2^{(i)})$$

and

$$H_2^{(i)}(P) = k_3^{(i)} H(k_3^{(i)} - P) + P \cdot H(P - k_3^{(i)}) \cdot H(k_4^{(i)} - P) + k_4^{(i)} H(P - k_4^{(i)}).$$

Here the function H is defined in the usual way by

$$H(x) = \begin{cases} 1, & \text{if } x > 0 \\ \frac{1}{2} & \text{if } x = 0 \\ 0, & \text{if } x < 0 \end{cases}.$$

Parameters $k_{1,2,3,4}^{(i)}$ are positive constants with $k_1^{(i)} < k_2^{(i)}$ and $k_3^{(i)} < k_4^{(i)}$. The growth function $g_1(C,P)$ of (8) is plotted in Figure 1 for a typical set of parameters that were estimated from laboratory experiments in [2] for a suspended culture of *Listeria monocytogenes* in vegetable broth. Moreover, for a probiotic strategy to be successful, the parameters must be such that the probiotics are more tolerant to protonated lactic acids and pH than the pathogen, e.g. $k_i^{(2)} \geq k_i^{(1)}, i = 1, \ldots, 4$ with a strict inequality for at least one i. Note from the equation for Y that, if $g_i(C,P) < 0$, active biomass N_i is converted into dead biomass, one-to-one.

Model (1)- (5) needs to be completed by proper boundary and initial conditions, see also below. For all practical purposes at time $t = 0$, biomass of type N_1 and of type N_2 will be located in sparsely distributed pockets along the substratum, i.e. along one side of the boundary of the domain. For the most part these pockets will be either populated by pathogens or by probiotics but not by both species at the same time. As long as the growth conditions in such a colony are everywhere favorable or in the neutral range, the model will behave locally like the single-species model of a pH controlled biofilm that was studied in [17]. Mixed colonies of both species will occur where such initially segregated neighboring colonies merge. We usually will assume that initially $Y \equiv 0$.

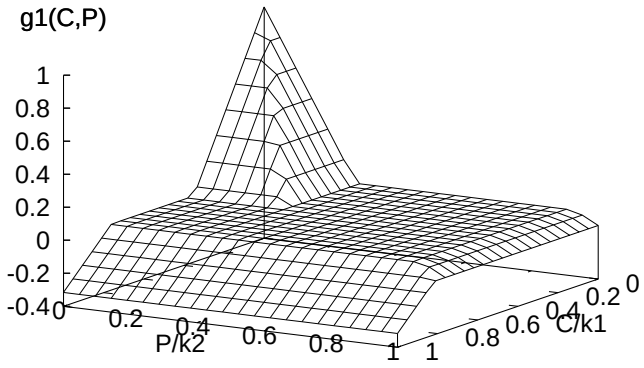

FIGURE 1. Growth function $g_1(C, P)$ for parameters that were determined in [2] for a suspended culture of *L. monocytogenes*.

.

3. **Existence result.** For our main result we consider model (1)-(5) with the Dirichlet boundary conditions

$$N_1\big|_{\partial\Omega} = N_2\big|_{\partial\Omega} = Y\big|_{\partial\Omega} = 0, \quad C\big|_{\partial\Omega} = C_r(x) \le k_1, \quad P\big|_{\partial\Omega} = P_r(x) \le k_2, \tag{9}$$

with non-negative $P_r, C_r \in L^\infty(\partial\Omega)$ and non-negative initial conditions

$$\begin{cases} C(0,\cdot) = C_0, \quad P(0,\cdot) = P_0, \quad N_1(0,\cdot) = N_{1,0}, \quad N_2(0,\cdot) = N_{2,0}, \quad Y(0,\cdot) = Y_0, \\ C_0, P_0, N_{1,0}, N_{2,0}, Y_0 \in L^\infty(\Omega), \\ \|N_{1,0} + N_{2,0} + Y_0\|_{L^\infty(\Omega)} = 1 - \delta_0 < 1, \\ 0 \le C_0 \le k_1, \quad 0 \le P_0 \le k_2, \quad 0 \le N_{1,0} + N_{2,0} + Y_0 \le 1 \end{cases} \tag{10}$$

where δ_0 is a positive constant between 0 and 1. We point out, however, that main result and proof carry over to more general boundary conditions as well, in a fashion similar to [15], where this was carried out for a single-species biofilm model.

Strictly speaking, the Dirichlet boundary conditions (9) describe "biofilms without substratum", i.e. (free floating) microbial flocs. Relevant for many practical purposes is also the case of a biofilm growing on a non-reactive impermeable substratum. The substratum is part of the boundary $\partial\Omega$, described by a hyperplane on which homogeneous Neumann conditions must hold. Boundary conditions (9) include this scenario by virtually extending the domain in a symmetric fashion about this hyperplane.

Before we prove the existence of solutions of (1)- (5) with (9) and (10), we make the following simple observation, which will be used below to obtain estimates.

Lemma 3.1. *The condition* $k_i^{(1)} < k_i^{(2)}$, $i = 1, \ldots, 4$ *implies that* $g_1(C, P) \le g_2(C, P)$, *where "=" holds only if* $g_1(C, P) = g_2(C, P) = 0$.

Proof. The assertion follows from the fact that the $g_i(C, P)$ are defined as monotonously decreasing, piecewise linear functions. We note that $H_1^{(1)}(C) \le$

$H_1^{(2)}(C)$ and $H_1^{(1)}(P) \le H_1^{(2)}(P)$. If $g_1(C,P) = 1 - C/H_1^{(1)}(C)$ and $g_2(C,P) = 1 - C/H_1^{(2)}(C)$, or $g_1(C,P) = 1 - P/H_2^{(1)}(P)$ and $g_2(C,P) = 1 - P/H_2^{(2)}(P)$, then the assertion follows directly. If $g_1(C,P) = 1 - P/H_2^{(1)}(P)$ and $g_2(C,P) = 1 - C/H_1^{(2)}(C)$, then we use $1 - P/H_2^{(1)}(P) \le 1 - C/H_1^{(1)}(C) \le 1 - C/H_1^{(2)}(C)$; similarly for the remaining case $g_1(C,P) = 1 - C/H_1^{(1)}(C)$, $g_2(C,P) = 1 - P/H_2^{(2)}(P)$. □

From this observation it follows directly that for the pathogens to grow faster than the probiotics $\mu_1 > \mu_2$ must hold necessarily.

We also will use the following Lemma about a non-degenerate regularization of a corresponding single-species pH-control model.

Lemma 3.2. *Let* $0 < \epsilon \ll 1$ *and*

$$D_{M,\epsilon}(M) = \begin{cases} d\frac{(M+\epsilon)^a}{(1-M)^b} & \text{if} \quad M \le 1-\epsilon \\ d\epsilon^{-b} & \text{if} \quad M > 1-\epsilon. \end{cases} \tag{11}$$

We consider the non-degenerate single species model

$$\partial_t C = \nabla \cdot (D_C(M)\nabla C) + \alpha M(k_1 - C), \tag{12}$$

$$\partial_t P = \nabla \cdot (D_P(M)\nabla P) + \alpha_3 C(k_2 - P), \tag{13}$$

$$\partial_t M = \nabla \cdot (D_{M,\epsilon}(M)\nabla M) + \mu g(C,P)M, \tag{14}$$

where $g(C,P)$ *is defined as in (8), with initial data*

$$\begin{cases} C(0,\cdot) = C_0, \quad P(0,\cdot) = P_0, \quad M(0,\cdot) = M_0 \\ C_0, P_0, M_0 \in L^\infty(\Omega), \\ \|M_0\|_{L^\infty(\Omega)} = 1 - \delta_0 < 1 \\ 0 \le C_0 \le k_1, \quad 0 \le P_0 \le k_3, \quad 0 \le M_0 \le 1 \end{cases}$$

and boundary conditions

$$M\big|_{\partial\Omega} = 0, \quad C\big|_{\partial\Omega} = C_r(x) < k_1, \quad P\big|_{\partial\Omega} = P_r(x) < k_2.$$

For every $t \ge 0$ *the solution* $(C(t), P(t), M(t))$ *of (12)-(14) satisfies*

$$0 \le C(t) \le k_1, \quad 0 \le P(t) \le k_2, \quad 0 \le M(t) \le 1 + \kappa\epsilon^b \tag{15}$$

for every small ϵ *and a* κ *that is independent of* ϵ.

Proof. The existence of a solution of the regularized second order parabolic system (12)-(14) is established in a classical manner if we can establish estimates on the L^∞ norm [18]. These can be obtained from the parabolic comparison principle.

Non-negativity of C, P, M follows by comparison with 0 and the upper estimates for C and P follow by comparison with the constant super-solutions $\bar{C} = k_1$ and $\bar{P} = k_2$. It remains to establish an upper estimate on M.

Let $m(x) \ge 0$ be the solution of the Dirichlet problem

$$\Delta m = -1, \quad m\big|_{\partial\Omega} = 0,$$

pick $\nu > 0$, and define the auxiliary function

$$M_\nu(x) := 1 + \nu m(x) \le 1 + \nu\tilde{\kappa},$$

where the constant $\tilde{\kappa}$ is an upper bound on m only and independent of ν. Then M_ν obviously gives upper bounds on the initial and boundary data of M. To show that this also is true for $t > 0$ and in all of Ω, we note that for sufficiently small ϵ the following inequality holds

$$\nabla_x \cdot (D_{M,\epsilon}(M_\nu)\nabla_x M_\nu) + \mu g(C,P)M_\nu \le -d\epsilon^{-b}\nu + 2\mu. \tag{16}$$

Picking now $\nu = \kappa'\epsilon$ with a constant $\kappa' \geq 2\mu/d$ we have

$$-d\epsilon^{-b}\nu + 2\mu \leq 0.$$

Thus, with (16), M_ν is a super-solution of (14) and the estimate

$$M(x,t) \leq M_\nu(x,t) \leq 1 + \kappa\epsilon^b$$

follows by comparison, where κ can be chosen as $\kappa = \tilde{\kappa}\kappa'$. □

Theorem 3.3. *The system (1)-(5) with boundary and initial conditions (9) and (10) possesses a solution in the sense of distributions in* $L^\infty(\mathbb{R}_+ \times \Omega) \times L^\infty(\mathbb{R}_+ \times \Omega) \times L^\infty(\mathbb{R}_+ \times \Omega) \times L^\infty(\mathbb{R}_+ \times \Omega) \times L^\infty(\mathbb{R}_+ \times \Omega)$.

Proof. The strategy to prove the assertion follows [4]. We study a non-degenerate approximation of the degenerate diffusion-reaction system (1)-(5) and show that its solution converges to a solution of the original problem.

We begin by showing that the initial-boundary value problem of the regularized, non-degenerate quasi-linear diffusion-reaction system

$$\begin{aligned}
\partial_t C &= \nabla \cdot (D_C(M)\nabla C) + \alpha_1 N_1(k_1 - C) + \alpha_2 N_2(k_1 - C), && (17)\\
\partial_t P &= \nabla \cdot (D_P(M)\nabla P) + \alpha_3 C(k_2 - P), && (18)\\
\partial_t N_1 &= \nabla\cdot(D_{M,\epsilon}(M)\nabla N_1) + \mu_1 g_1(C,P)N_1, && (19)\\
\partial_t N_2 &= \nabla\cdot(D_{M,\epsilon}(M)\nabla N_2) + \mu_2 g_2(C,P)N_2, && (20)\\
\partial_t Y &= \nabla\cdot(D_{M,\epsilon}(M)\nabla Y) - \mu_1 \min(0, g_1(C,P)N_1) - \mu_2 \min(0, g_2(C,P)N_2) && (21)
\end{aligned}$$

possesses a solution, where $D_{M,\epsilon}(M)$ is defined as in (11).

We denote these solutions by $(C_\epsilon, P_\epsilon, N_{1,\epsilon}, N_{2,\epsilon}, Y_\epsilon)$. From the positivity criterion for quasilinear parabolic systems in [4] it can be concluded that these solutions, if they exist, are non-negative. In order to show the existence of these solutions it suffices, again with the familiar arguments [18], to establish L^∞ *a priori* estimates. We define

$$M_\epsilon := N_{1,\epsilon} + N_{2,\epsilon} + Y_\epsilon$$

and add the equations for the biomass fractions to obtain

$$\begin{aligned}
\partial_t M_\epsilon = \nabla\cdot(D_{M,\epsilon}(M_\epsilon)\nabla M_\epsilon) &+ \mu_1 \max(0, g_1(C_\epsilon, P_\epsilon)N_{1,\epsilon})\\
&+ \mu_2 \max(0, g_2(C_\epsilon, P_\epsilon)N_{2,\epsilon}).
\end{aligned} \tag{22}$$

We introduce the notation

$$k_\epsilon := \mu \max(0, g_2(C_\epsilon, P_\epsilon)), \qquad \mu := \max\{\mu_1, \mu_2\}$$

and obtain with Lemma 3.1 and with $Y_\epsilon \geq 0$, which was established above, the differential inequality

$$\partial_t M_\epsilon \leq \nabla\cdot(D_{M,\epsilon}(M_\epsilon)\nabla M_\epsilon) + k_\epsilon M_\epsilon.$$

The solution $\bar{M}_\epsilon$ of the associated differential equation,

$$\partial_t \bar{M}_\epsilon = \nabla\cdot\big(D_{M,\epsilon}(\bar{M}_\epsilon)\nabla\bar{M}_\epsilon\big) + k_\epsilon\bar{M}_\epsilon$$

is an upper estimate for M_ϵ, i.e. $\bar{M}_\epsilon(t,x) \geq M_\epsilon(t,x)$, cf. (14) and Lemma 3.2. Thus, there exists a constant K_ϵ^* such that

$$0 \leq M_\epsilon \leq K_\epsilon^*$$

and, hence, due to non-negativity the *a priori* estimates

$$0 \leq N_{1,\epsilon}, N_{2,\epsilon}, Y_\epsilon \leq K_\epsilon^*.$$

This establishes the existence of solutions. Note that $K_\epsilon^* \to 1$ as $\epsilon \to 0$.

Next we show that the solutions of the regularized system (17)-(21) converge as $\epsilon \to 0$. Similar as in [5, 15, 17] we write the spatial diffusion operator in terms of the Laplacian, instead of the divergence form, i.e. we introduce the functions

$$\Phi_\epsilon(M) := \int_0^M D_{M,\epsilon}(s)ds.$$

Due to $b \geq 1$ we have $\lim_{\epsilon\to 0} \Phi_\epsilon(1) = \infty$. Since $M_\epsilon(t,x) \leq \gamma$ for a γ that depends only on the initial data (more specifically, on δ_0 [15]), we can find a β_γ such that $\Phi_\epsilon(M_\epsilon(t,x))$ is uniformaly bounded from above and below for all sufficiently small ϵ, i.e.

$$0 \leq \Phi_\epsilon(M_\epsilon(t,x)) < \beta_\gamma < \infty.$$

On the parabolic cylinder $Q_T := (T, T+1] \times \Omega$ for fixed T, our M_ϵ satisfies the equation

$$\partial_t M_\epsilon = \Delta\Phi_\epsilon(M_\epsilon) + h_\epsilon,$$

where $h_\epsilon := \mu_1 \max(0, g_1(C_\epsilon, P_\epsilon)N_{1,\epsilon}) + \mu_2 \max(0, g_2(C_\epsilon, P_\epsilon)N_{2,\epsilon})$. As shown above, the parabolic operator in this equation is regular and $h_\epsilon \in L^\infty(Q_T)$. Therefore, the classical theory [18] of quasilinear parabolic equations ensures $M \in \mathcal{C}^\alpha(Q_T)$ for some $\alpha > 0$ and

$$\|M_\epsilon\|_{\mathcal{C}^\alpha(Q_T)} \leq q\left(\|h_\epsilon)\|_{L^\infty(Q_T)}\right),$$

where q is a non-decreasing function that depends on the upper and lower bounds on Φ_ϵ that were established above. Furthermore, since $\|h_\epsilon\|$ is uniformly bounded (relatively to ϵ), M_ϵ is bounded in $\mathcal{C}^\alpha(Q_T)$, which is compactly embedded in $\mathcal{C}(\overline{Q_T})$. Therefore, as $\epsilon \to 0$, M_ϵ converges strongly in $\mathcal{C}(Q_T)$-norm to some $M_* \in \mathcal{C}(\overline{Q_T})$. Since $N_{1,\epsilon}$, $N_{2,\epsilon}$, Y_ϵ are uniformly bounded under the $L^\infty(Q_T)$ norm, it follows the existence of a sequence ϵ_n ($\epsilon_n \to 0$), for which N_{1,ϵ_n}, N_{2,ϵ_n}, Y_{ϵ_n} converge weakly in $L^2(Q_T)$ to some $N_{1,*}$, $N_{2,*}$, Y_*. Thus, $M_{\epsilon_n} = N_{1,\epsilon_n} + N_{2,\epsilon_n} + Y_{\epsilon_n}$ converges weakly to $N_{1,*} + N_{2,*} + Y_*$. Thus, $M_* = N_{1,*} + N_{2,*} + Y_*$.

It remains to show that the limits $N_{1,*}$, $N_{2,*}$, Y_* are indeed (weak) solutions of our original degenerate equations. The method of proof is the same for each of those, so we will show it for one only, namely $N_{1,*}$. As a weak solution, $N_{1,*}$ has to satisfy

$$\begin{aligned} &\int_\Omega N_{1,*}(T+1,x)\varphi(x)dx - \int_\Omega N_{1,*}(T,x)\varphi(x)dx = \\ &\int_{Q_T} \nabla\left(D_M(M_*)\nabla N_{1,*}\right)\varphi(x)dxdt + \int_{Q_T} \mu_1 g_1(C_*,P_*)N_{1,*}\varphi(x)dxdt \end{aligned} \tag{23}$$

for all test functions $\varphi \in \mathcal{D}(\Omega)$, where $\mathcal{D}(\Omega)$ is, in the usual way, the set of all infinitely differentiable functions over Ω with compact support. We consider

$$\begin{aligned} &\int_\Omega N_{1,\epsilon}(T+1,x)\varphi(x)dx - \int_\Omega N_{1,\epsilon}(T,x)\varphi(x)dx = \\ &\int_{Q_T} \nabla\left(D_{M,\epsilon}(M_\epsilon)\nabla N_{1,\epsilon}\right)\varphi(x)dxdt + \int_{Q_T} \mu_1 g_1(C_\epsilon,P_\epsilon)N_{1,\epsilon}\varphi(x)dxdt \end{aligned} \tag{24}$$

and pass ϵ to the limit in order to establish (23). Obviously for $\epsilon \to 0$,

$$\begin{aligned} \textstyle\int_\Omega N_{1,\epsilon}(T+1,x)\varphi(x)dx &\longrightarrow \textstyle\int_\Omega N_{1,*}(T+1,x)\varphi(x)dx, \\ \textstyle\int_\Omega N_{1,\epsilon}(T,x)\varphi(x)dx &\longrightarrow \textstyle\int_\Omega N_{1,*}(T,x)\varphi(x)dx, \\ \textstyle\int_{Q_T} \mu_1 g_1(C_\epsilon,P_\epsilon)N_{1,\epsilon}\varphi(x)dxdt &\longrightarrow \textstyle\int_{Q_T} \mu_1 g_1(C_*,P_*)N_{1,*}\varphi(x)dxdt. \end{aligned} \tag{25}$$

In order to confirm that this is also so for the remaining term in (23), we show first the strong convergence of $D_{M,\epsilon}(M_\epsilon)$ to $D_M(M_*)$. To do this we construct an upper bound (uniform, relatively to ϵ) on M_ϵ by comparison. Similar as in Lemma 3.2 we consider the auxiliary linear elliptic Poisson problem

$$\Delta V = -K_1, \quad V|_{\partial\Omega} = K_2 \tag{26}$$

where the constant K_1 is defined as

$$K_1 := \sup_{\epsilon>0} \|h_\epsilon\|_{L^\infty(\mathbb{R}_+,\Omega)}$$

and K_2 as

$$K_2 := \sup_{\epsilon>0} \|\Phi_\epsilon(M_0)\|_{L^\infty(\Omega)}$$

with $M_0 := N_{1,0} + N_{2,0} + Y_0$. Recall that $\|M_0\|_{L^\infty(\Omega)} < 1 - \delta_0$ for some $0 < \delta_0 < 1$ per hypothesis. Thus, also K_2 depends only on δ_0. The solution of the regular elliptic problem (26) is bounded over Ω. For small enough ϵ we define for all $t > 0$

$$Z_\epsilon(t,x) := \Phi_\epsilon^{-1}(V(x)).$$

Obviously Z_ϵ is in equilibrium, $\partial_t Z \equiv 0$, and we have the inequality

$$\partial_t Z - \Delta\Phi_\epsilon(Z_\epsilon) = K_1 \geq h_\epsilon = \partial_t M_\epsilon - \Delta\Phi_\epsilon(M_\epsilon),$$

as well as

$$M_\epsilon|_{\partial\Omega} = 0 \leq Z_\epsilon|_{\partial\Omega} = \Phi_\epsilon^{-1}(K_2)$$

for the boundary values and for the initial data

$$M_\epsilon(0,x) \leq Z_\epsilon(0,x), \quad x \in \Omega.$$

From these three inequalities we derive with the parabolic comparison principle that for small enough ϵ

$$M_\epsilon(t,x) \leq Z_\epsilon(t,x), \quad \text{for all} \quad t \geq 0, x \in \Omega. \tag{27}$$

Moreover, since $V(x)$ is bounded, there is an ϵ_* such that for $\epsilon < \epsilon_*$

$$Z_\epsilon(t,x) \leq \Phi_\epsilon^{-1}\left(\sup_{x\in\Omega} V(x)\right), \qquad \sup_{0<\epsilon<\epsilon_*} \Phi_\epsilon^{-1}\left(\sup_{x\in\Omega} V(x)\right) < 1.$$

This shows the uniform boundedness (with respect to ϵ) of the family of functions M_ϵ by a constant strictly smaller than unity, implying the strong convergence of $D_{M,\epsilon}(M_\epsilon)$ to $D_M(M_*)$ in $\mathcal{C}(Q_T)$. To finalize the proof we need to show that the remainder

$$R_\epsilon := \int_{Q_T} D_M(M_*)\nabla N_{1,*}\nabla\varphi dx - \int_{Q_T} D_{M,\epsilon}(M_\epsilon)\nabla N_{1,\epsilon}\nabla\varphi(x)dx \tag{28}$$

vanishes for vanishing ϵ, where we used integration by parts to re-write the remaining terms of (23) and (24). We define for $0 < \delta < 1$ the open set (due to continuity of M_*)

$$Q_{T,\delta} := \{(t,x) \in Q_T : M_*(t,x) < \delta\}.$$

and decompose R_ϵ of $Q_{T,\delta}$ and its complement $Q^c_{T,\delta}$,

$$R_\epsilon = I_\epsilon(\delta) + J_\epsilon(\delta)$$

with

$$I_\epsilon(\delta) := \int_{Q_{T,\delta}} D_M(M_*)\nabla N_{1,*}\nabla\varphi dxdt - \int_{Q_{T,\delta}} D_{M,\epsilon}(M_\epsilon)\nabla N_{1,\epsilon}\nabla\varphi(x)dxdt$$

and

$$J_\epsilon(\delta) := \int_{Q^c_{T,\delta}} D_M(M_*)\nabla N_{1,*}\nabla\varphi dxdt - \int_{Q^c_{T,\delta}} D_{M,\epsilon}(M_\epsilon)\nabla N_{1,\epsilon}\nabla\varphi(x)dxdt.$$

Note that R_ϵ is independent of δ and that it vanishes if both $I_\epsilon(\delta)$ and $J_\epsilon(\delta)$ vanish. We will first obtain an estimate on $I_\epsilon(\delta)$. Multiplying equation (19) by $N_{1,\epsilon}$ and integrating over Ω gives

$$\frac{d}{dt}\|N_{1,\epsilon}(t)\|^2_{L^2(\Omega)} = -\int_\Omega D_{M,\epsilon}(M_\epsilon)|\nabla N_{1,\epsilon}|^2dx + \int_\Omega g_\epsilon N_{1,\epsilon}dx,$$

where we used g_ϵ as short-hand notation

$$g_\epsilon := \mu_1 g_1(C_\epsilon, P_\epsilon)N_{1,\epsilon}.$$

After integrating also over t from T to $T+1$ we have

$$\begin{aligned}&\|N_{1,\epsilon}(T+1)\|^2_{L^2(\Omega)} + \int_{Q_T} D_{M,\epsilon}(M_\epsilon)|\nabla N_{1,\epsilon}|^2dxdt\\ &= -\int_{Q_T} g_\epsilon N_{1,\epsilon}dxdt + \|N_{1,\epsilon}(T)\|^2_{L^2(\Omega)}\end{aligned}$$

and, therefore,

$$\int_{Q_T} D_{M,\epsilon}(M_\epsilon)|\nabla N_{1,\epsilon}|^2dxdt \le -\int_{Q_T} g_\epsilon N_{1,\epsilon}dxdt + \|N_{1,\epsilon}(T)\|^2_{L^2(\Omega)} \tag{29}$$

The term on the right hand side of (29) is uniformly bounded by some K independently of ϵ. Moreover, we can write

$$D_{M,\epsilon}(M_\epsilon)\nabla N_{1,\epsilon} = \sqrt{D_{M,\epsilon}(M_\epsilon)}\sqrt{D_{M,\epsilon}(M_\epsilon)}\nabla N_{1,\epsilon}$$

and, thus, have shown

$$\|\sqrt{D_{M,\epsilon}(M_\epsilon)}\nabla N_{1,\epsilon}\|_{L^2(Q_T)} \le K. \tag{30}$$

From the Hölder inequality for the first integral in $I_\epsilon(\delta)$ we obtain the estimate

$$\left(\int_{Q_T}\sqrt{D_{M,\epsilon}(M_\epsilon)}\nabla N_{1,\epsilon}\sqrt{D_{M,\epsilon}(M_\epsilon)}\nabla\varphi dxdt\right)^2 \le K_1^2\int_{Q_{T,\delta}}\frac{d(M_\epsilon+\epsilon)^a}{(1-M_\epsilon)^b}|\nabla\varphi|^2dxdt.$$

On $Q_{T,\delta}$ the estimate $M_* < \delta$ holds. Therefore, there is an $\epsilon_0 > 0$ such that for all sufficiently small $\epsilon < \epsilon_0$ the estimate $M_\epsilon \le 2\delta$ holds and, thus,

$$I_\epsilon(\delta) \le K_2\frac{(3\delta)^a}{K_3^b}\|\varphi\|_{H^1(\Omega)}, \tag{31}$$

where constant K_2 subsumes d and K_1 from above and constant K_3 is an estimate on $1-M_\epsilon$ according to (27).

Next we estimate $J_\epsilon(\delta)$ for $\delta > 0$, i.e we need to show that

$$\nabla N_{1,\epsilon} \rightharpoonup \nabla N_{1,*} \text{ in } L^2(Q^c_{T,\delta}). \tag{32}$$

For given δ, there is an ϵ_1, such that for $\epsilon < \epsilon_1$

$$d\left(\frac{\delta}{2}\right)^a \le D_{M,\epsilon}(M_\epsilon)$$

on $Q^c_{T,\delta}$ and, thus, with (30)

$$\int_{Q^c_{T,\delta}} |\nabla N_{1,\epsilon}|^2 dxdt \leq \frac{K'}{\delta^a}.$$

The constant K' is independent of ϵ. This implies weak-convergence for a subsequence in $L^2(Q^c_{T,\delta})$, i.e. weak convergence to some $\xi \in L^2(Q^c_{T,\delta})$. Moreover, $\nabla N_{1,\epsilon}$ converges in $\mathcal{D}'(Q^c_{T,\delta})$ to $\nabla N_{1,*}$, because of the uniform convergence in $\mathcal{C}(\overline{Q^c_{T,\delta}})$. The limit in $\mathcal{D}'(Q^c_{T,\delta})$ is unique and, thus, we obtain the weak convergence of $\nabla N_{1,\epsilon}$ to $\nabla N_{1,*}$ over $Q^c_{T,\delta}$, i.e. we proved (32).

From the strong convergence of $D_{M,\epsilon}(M_\epsilon)$ to $D_M(M_*)$ and from the weak convergence of $\nabla N_{1,\epsilon}$ to $\nabla N_{1,*}$, we obtain finally for every $\delta > 0$,

$$\lim_{\epsilon \to 0} J_\epsilon(\delta) = 0.$$

To finish the proof, let us pick an $\eta > 0$. Due to (31) there exist for this η a δ_η and an $\epsilon_{0,\eta}$ such that $I_\epsilon(\delta_\eta) \leq \frac{\eta}{2}$ for $\epsilon < \epsilon_{0,\eta}$, i.e. for small enough ϵ. Moreover, since $J_\epsilon(\delta) \to 0$, there is also an $\epsilon_{1,\eta}$ such that $J_\epsilon(\delta) \leq \frac{\eta}{2}$ for $\epsilon < \epsilon_{1,\eta}$. $R_\epsilon = I_\epsilon(\delta) + J_\epsilon(\delta)$ is independent of δ. Thus for every $\eta > 0$ a ϵ_η exists with $\epsilon_\eta := \min\{\epsilon_{0,\eta}, \epsilon_{1,\eta}\}$, such that $R_\epsilon \leq \eta$ for $\epsilon \leq \epsilon_\eta$. Thus R_ϵ vanishes. Together with (25) this proves that indeed $N_{1,*}$ satisfies (23). The same procedure can be carried out for the remaining components of the solution and the the assertion in proved. □

Remark 1. Note that we are only able to establish the existence of solutions of the initial-boundary value problem (1)-(5), (9), (10). Unlike in the case of the prototype biofilm model with but one particular substance [15], i.e one volume occupying biomass fraction, we do not have a uniqueness result for the multi-species system. Neither do we have a non-uniqueness result.

4. Simulation experiment.

4.1. Computational setup.

To demonstrate the qualitative behavior of the solutions of model (1)-(5) we conduct numerical simulations. In [25] it was shown for some typical problems that for biofilm systems that are driven by mass transfer only, two-dimensional simulations can capture the behavior of more realistic, but also computationally much more expensive, three-dimensional systems very well. Therefore, as domain we choose the interval $\Omega = [0, L] \times [0, H]$, with the boundary segment $x_2 = 0$ as substratum.

The discretization of the governing equations follows the strategy that was outlined and analyzed for a mono-culture biofilms in [6]. For that purpose the domain Ω is discretized by a uniform mesh of 200×160 computational cells. The key element of the algorithm is a non-local (in time) discretization in the fashion of Non-standard Finite Difference Schemes [1, 20], i.e. nonlinear diffusion and reaction terms are represented by approximations from two sub-sequent time-levels. This leads to a semi-implicit method that requires the solution of a sparse linear system for each of the five dependent variables in every time-step. To this end we use the stabilized biconjugate gradient method. The algorithm has been implemented in Fortran 90. For the linear solver we use the Fortran 77 source code library SPARSKIT [22] that is based on reverse communication. The linear solver and the evaluation of the nonlinear reaction terms as computationally most intensive parts of the code have been parallelized for execution on shared memory computers using OpenMP. For our simulations we used a SGI ALTIX 450 compute server with 32 dual core Itanium

II processors, running SUSE Linux and the Intel Fortran compiler. After efficiency consideration and testing, computations were conducted using four parallel threads each, thus allowing to run multiple parallel compute jobs concurrently.

Along the substratum $x_2 = 0$ homogeneous Neumann conditions hold for all dependent variables. Homogeneous Neumann conditions are also specified everywhere else on $\partial\Omega$ for the biomass fractions N_1, N_2, Y. For the dissolved substrates C, P we specify homogeneous Neumann conditions at the lateral boundaries $x_1 = 0$ and $x_1 = L$ and Dirichlet conditions at the top boundary $x_2 = H$. Note that this change in boundary conditions does not affect the existence result. The required properties for C and P carry over to mixed boundary value problems, cf. also [15]. These boundary conditions were chosen for the simulations because they appear more natural for most applications.

In every simulation, initially pathogenic and probiotic biomass can only be found in few pockets along the substratum, i.e. in selected cells along $x_2 = 0$. Everywhere else $N_1 = 0$ and $N_2 = 0$ initially. The number of such biomass pockets is specified on input but their actual location is chosen randomly (uniformly distributed). Each pocket has initially a size of 2×2 grid cells. In the simulations reported here we inoculate with 15 pathogenic pockets and 5 control agent pockets. The actual biomass density in these pockets is also chosen randomly, namely uniformly distributed between 0.5 and 0.7. Initially, no inert biomass is in the system, $Y_0 \equiv 0$. For the dissolved substrates C and P we choose constant initial data C_0 and P_0. More specific, these values are chosen as the Dirichlet values. We pick them small enough to be in the growth range for both species.

4.2. **Simulations.**

4.2.1. *Pathogen growth limitations (parameter set I).* The development of a dual-species biofilm that is formed by a pathogen and a (probiotic) biocontrol agent is visualized in Figure 2. The parameters used in this simulation are listed in Table 1 as parameter set I. The biofilm growth parameters are adapted from typical values in the literature. The control kinetics parameters have been adapted from [2].

Initially the individual colonies are separated but they expand in an initial growth phase that leads to a merging of neighboring colonies into bigger colonies, which might be inhabited by both species. Although the maximum growth rate is lower for the control agent than for the pathogen, and although initially three times as many pathogens were in the system than control-agents, the control agents eventually starts dominating the system, because they are more tolerant to the growth inhibitors.

Note that here for both species the stationary phase is reached rather early, i.e. $k_{1,3}^{(1,2)}$ are relatively small. This implies that biofilm growth quickly comes to a slow down. The biofilm remains rather small and patchy. Moreover, the stationary range is quite extended, because the decay concentrations are rather large. In our simulation the decay phase is never reached, i.e. $Y \equiv 0$ throughout. In fact, the pathogenic biomass remains virtually unchanged over a long period of time, while the probiotic biomass keeps growing at the outer rims of the biofilm colonies, where growth conditions are still favorable, although slowing down there as well. All growth in and expansion of the biofilm for large time is entirely due to the production of new viable biocontrol agent.

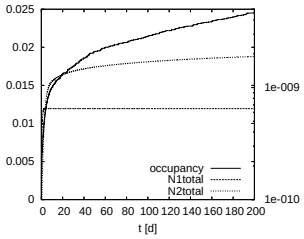

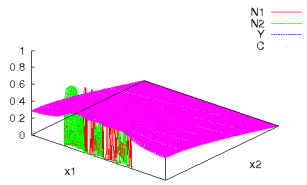

$t = 4$d

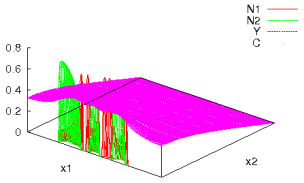

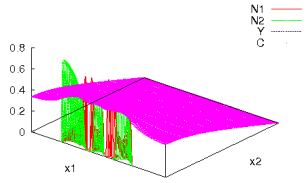

$t = 9$d $t = 14$d

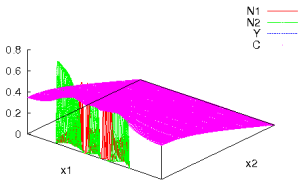

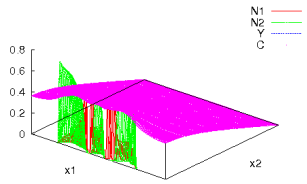

$t = 24$d $t = 49$d

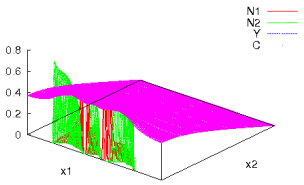

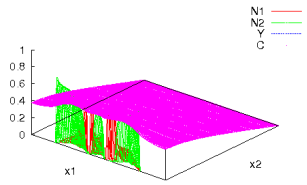

$t = 74$d $t = 99$d

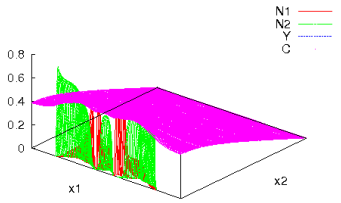

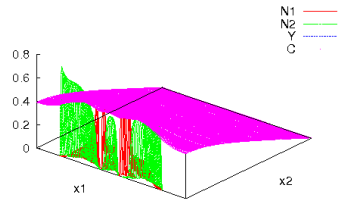

$t = 149$d $t = 174$d

FIGURE 2. Simulation of model (1)-(5) for the parameter set I (pathogen growth limitation). The top left panel shows the lumped parameters biofilm occupancy $\omega(t)$ and total biomass $N_{1,total}(t)$, $N_{2,total}$. Plotted are the solution surfaces $N_1(t,\cdot)$, $N_2(t,\cdot)$, $Y(t,\cdot)$ and $C(t,\cdot)$ for selected time instances t.

TABLE 1. Model parameters used in the computer simulations. Protonated acid concentrations and hydrogen ion concentrations are normalised with respect to saturation values k_1 and k_2, respectively.

Parameter	**Symbol**	**Value I** (limitation)	**Value II** (eradication)	**Unit**
length of domain	L	$0.5{\cdot}10^{-3}$	$0.5{\cdot}10^{-3}$	m
height of domain	H	$0.4{\cdot}10^{-3}$	$0.4{\cdot}10^{-3}$	m
max. growth rate, pathogens	μ_1	3	3	1/d
max. growth rate, probiotics	μ_2	2.5	2.5	1/d
acid production rate, pathogens	α_1	4000	4000	1/d
acid production rate, probiotics	α_2	7000	7000	1/d
hydrogen ions production rate	α_3	10	10	1/d
acid saturation level	k_1	1	1	–
hydrogen ion saturation level	k_2	1	1	–
pathogen growth kinetics	$k_1^{(1)}$	0.35	0.86	–
	$k_2^{(1)}$	0.76	0.89	–
	$k_3^{(1)}$	0.275	0.80	–
	$k_4^{(1)}$	0.93	0.86	–
probiotic growth kinetics	$k_1^{(2)}$	0.45	0.89	–
	$k_2^{(2)}$	0.76	0.94	–
	$k_3^{(2)}$	0.52	0.82	–
	$k_4^{(2)}$	0.93	0.86	–
bulk concentration, C	C_0	0	0	–
bulk concentration, P	P_0	0.0033	0.0033	–
diffusion coefficient, C in biofilm	$D_C(1)$	$10\cdot 10^{-6}$	$10{\cdot}10^{-6}$	m^2/d
diffusion coefficient, C in water	$D_C(0)$	$7.0\cdot 10^{-6}$	$7.0{\cdot}10^{-6}$	m^2/d
diffusion coefficient, P in biofilm	$D_P(1)$	$5.0\cdot 10^{-6}$	$5.0{\cdot}10^{-6}$	m^2/d
diffusion coefficient, P in water	$D_P(0)$	$4.95{\cdot}10^{-6}$	$4.95{\cdot}10^{-6}$	m^2/d
biofilm interface exponent	a	4	4	–
biofilm threshold exponent	b	4	4	–
biofilm motility coefficient	d	$81{\cdot}10^{-12}$	$81{\cdot}10^{-12}$	m^2/d

In support of these observations we plot in Figure 2 also the total biomass fractions

$$N_{1,total}(t)=\int_\Omega N_1(t,x)dx,\ N_{2,total}(t)=\int_\Omega N_2(t,x)dx,\ Y_{total}(t)=\int_\Omega Y(t,x)dx,$$

in the system, as well as the dimensionless biofilm size

$$\omega(t)=\frac{\int_{\Omega_2(t)}dx}{\int_\Omega dx} \tag{33}$$

i.e. the fraction of the domain Ω that is occupied by biomass.

The limiting substrate in this simulation is the protonated lactic acid concentration C, while the hydrogen ion concentration remains in a favorable range throughout. The growth limiting substrates are highest close to the substratum, i.e. the conditions are worst for the bacteria in the inner layers of the biofilm.

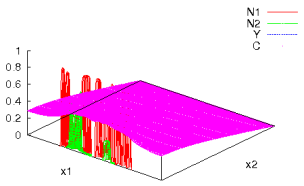

$t = 1$d

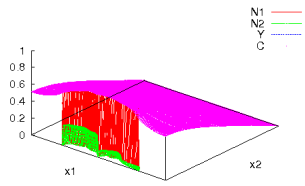

$t = 2.5$d

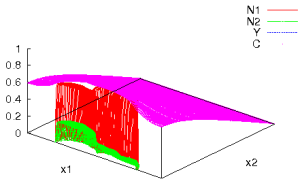

$t = 4$d

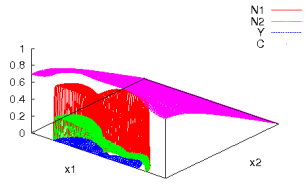

$t = 9$d

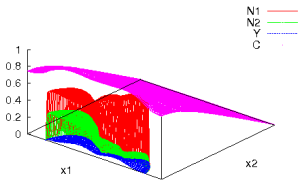

$t = 14$d

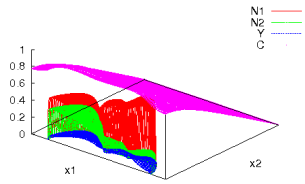

$t = 19$d

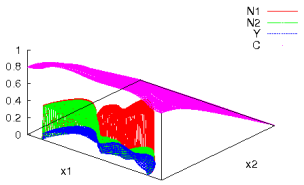

$t = 24$d

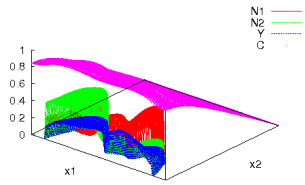

$t = 34$d

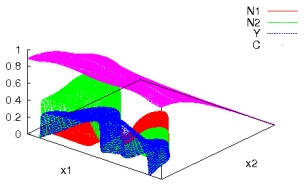

$t = 44$d

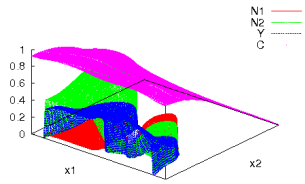

$t = 49$d

FIGURE 3. Simulation of model (1)-(5) for the parameter set II (eradication of pathogens). Plotted are the solution surfaces $N_1(t,\cdot)$, $N_2(t,\cdot)$, $Y(t,\cdot)$ and $C(t,\cdot)$ for selected time instances t.

4.2.2. *Pathogen eradication (parameter set II).* A second simulation is shown in Figure 3. Compared to the previous simulation, the growth controlling parameters $k_j^{(i)}, j = 1, 3, i = 1, 2$ have been increased, cf. parameter value set II in Table 1. The parameters $k_2^{(i)}$, $i = 1, 2$ have been increased, $k_4^{(i)}$, $i = 1, 2$ have been decreased. These parameters determine the transition into the decay phase. Thus, the growth phase is longer and the stationary phase is reached later. This allows for the formation of a thicker biofilm.

As in the previous simulation the initially separated colonies merge into bigger multi-species colonies. However, since both species are more tolerant to the growth limiters than in the previous simulation, this expansion and merging phase is prolonged. Eventually all biomass is organized in two such large colonies. Initially the faster growing pathogens dominate both colonies but eventually, when the protonated lactic acid concentration reaches the stationary and decay range, production of the pathogen slows down and the biocontrol agents become dominating in one of the two colonies. This is a consequence of continuing growth of the control agents (because they are more tolerant to the growth limiters), as well as of an actual decrease of pathogens because of inactivation of the pathogen due to high concentration values C. The other, smaller, colony remains longer dominated by the pathogens. Alas, also there eventually inactivation occurs and the pathogens decrease while the control agents still increase.

Furthermore, the stationary phase in this case is not as extended. In fact the decay phase starts quickly after the stationary phase is reached. As the visualizations show, eventually more inert biomass can be found in the colonies than pathogens. Later also the control agent becomes inactivated, i.e. transformed into inert biomass, albeit a lower rate.

The simulations in Figure 3 clearly show that inert biomass accumulates first in the inner layers of the biofilm, close to the substratum, while the bacteria closer to the biofilm/liquid interface live longer under favorable conditions. This is expected, since the detrimental substrates are produced in the biofilm and diffuse out of it. It should be pointed out, however, that this behavior is quite contrary to the situation in antibiotic biofilm control, where the bacteria at the biofilm/liquid interface are hit hardest, while the cells in the inner regions can survive longer [4]. Both effects are explained by reactions and diffusive resistance in the biofilm matrix, i.e. are characteristic for biofilms but not for planktonic communities.

In Figure 4 the total biomass fractions and the biofilm occupancy are plotted as functions of time for a developing biofilm. While the underlying model equations are fully deterministic, the initial inoculation is chosen randomly. In order to qualify the effect of this random component on the lumped parameters above, we include the data of 13 simulations in Figure 4. We find that the results of these simulations are in good agreement with each other. The plots of the lumped functions confirm the findings above: The biofilm keeps growing over the entire simulation period. This is due to a continued growth of the probiotic population, while the pathogenic population eventually is diminished, i.e. converted into inactive biomass, after passing through its maximum. This coincides naturally with an increase of inert biomass.

5. **Conclusion.** We presented a mathematical model for the amensalistic control of a pathogenic biofilm by lactic acid biofilm formers. In numerical simulations we illustrated the workings of this bio-control mechanism. In particular it was shown

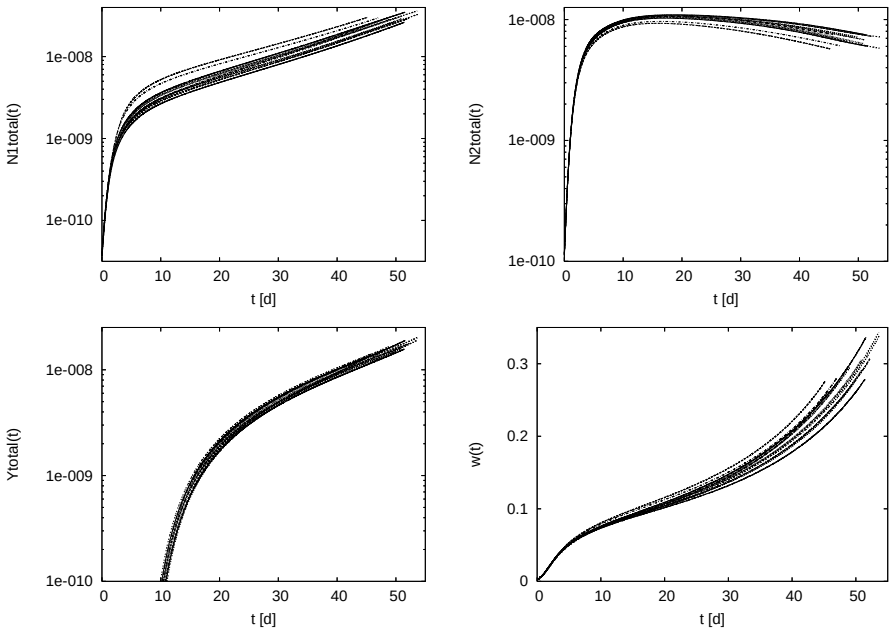

FIGURE 4. Lumped parameters total biomass and biofilm size for an evolving biofilm as function of time. The parameters are the same as in Figure 3

that pathogens are eradicated first in the deeper layers of the biofilm, close to the substratum, whereas in traditional antibiotic biofilm control first the cells in the outer layers are deactivated. These simulations will be extended by accounting for convective contributions to transport of dissolved substrates in the liquid phase in a forthcoming study [12].

From a more mathematical point of view, we could give an existence proof for the resulting degenerated mixed-culture biofilm model. Neither a uniqueness nor a non-uniqueness result was obtained. This naturally poses a question for further mathematical research in this area.

Acknowledgments. HJE acknowledges financial support received from the *Canada Research Chairs Program* (CRC) and the *Natural Science and Engineering Research Council of Canada* (NSERC). Simulations have been carried out on a SGI ALTIX compute server funded by the Canada Foundation for Innovation (CFI) and the Ontario Ministry of Research and Innovation. We thank the staff at SHARCNET (the Shared Hierarchic Academic Research Network) for their effort in maintaining and operating this machine.

REFERENCES

[1] R. Anguelov and J. M. S. Lubuma, *Contributions to the mathematics of the nonstandard finite difference method and its applications*, Num. Meth. PDE., **17** (2001), 518–543.

[2] F. Breidt and H. P. Flemming, *Modeling of the competitive growth of Listeria monocytogenes and Lactococcus lactis in vegetable broth*, Appl. Env. Microbiol., **64(9)** (1998), 3159–3165.

[3] CIHR Institute of Infection and Immunity (III), *Novel Alternatives to Antibiotics*, Workshop Report, available at http://www.cihr-irsc.gc.ca/e/27879.html, 2005.

[4] L. Demaret, H. Eberl, M. Efendiev and R. Lasser, *Analysis and simulation of a meso-scale model of diffusive resistance of bacterial biofilms to penetration of antibiotics*, Adv. Math. Sc. and Appls., **18(1)** (2008), 269–304.
[5] A. Duvnjak and H. J. Eberl, *Time-discretisation of a degenerate reaction-diffusion equation arising in biofilm modeling*, El. Trans. Num. Analysis, **23** (2006), 15–38.
[6] H. J. Eberl and L. Demaret, *A finite difference scheme for a doubly degenerate diffusion-reaction equation arising in microbial ecology*, El. J. Diff. Equ. CS, **15** (2007), 77–95.
[7] H. Eberl, D. Parker and M. van Loosdrecht, *A new deterministic spatio-temporal continuum model for biofilm development*, J. Theor. Medicine, **3(3)** (2001), 161–176.
[8] H. J. Eberl and M. A. Efendiev, *A transient density dependent diffusion-reaction model for the limitation of antibiotic penetration in biofilms,* El. J. Diff. Eq. CS, **10** (2003), 123–142.
[9] H. J. Eberl, *A deterministic continuum model for the formation of EPS in heterogeneous biofilm architectures*, Biofilms 2004, Las Vegas, Nv.
[10] H. J. Eberl and H. Schraft, *A diffusion-reaction model of a mixed culture biofilm arising in food safety studies*, in *Mathematical modeling of biological system, Vol. II*, A. Deutsch et al, eds, Birkhäuser (2007), 109–120.
[11] H. J. Eberl and R. Sudarsan, *Exposure of biofilms to slow flow fields: the convective contribution to growth and disinfections*, J. Theor. Biol., **253(4)** (2008), 788–807.
[12] H. J. Eberl, H. Khassehkhan and L. Demaret, *A mixed-culture model of a probiotic biofilm control system*, Comp. Math. Meth. Med., *to appear*
[13] M. A. Efendiev and L. Demaret, *On the structure of attractors for a class of degenerate reaction-diffusion systems*, Adv. Math. Sci. & Appls., **18** (2008), 105–118.
[14] M. A. Efendiev, H. J. Eberl and S. V. Zelik, *Existence and longtime behavior of solutions of a nonlinear reaction-diffusion system arising in the modeling of biofilms*, RIMS Kokyuroko, **1258** (2002), 49–71.
[15] M. A. Efendiev, S. V. Zelik and H. J. Eberl, *Existence and longtime behavior of a biofilm model*, Comm. Pure Appl. Analysis, **8(2)** (2009), 509–531.
[16] FAO/WHO Working Group, "Guidelines for the Evaluation of Probiotics in Food," FAO/WHO, London, On, 2002.
[17] H. Khassehkhan and H. J. Eberl, *Modeling and simulation of a bacterial biofilm that is controlled by pH and protonated lactic acids*, Comp. Math. Meth. Med., **9(1)** (2008), 47–67.
[18] O. Ladyzhenskaya, O. Solonnikov and N. Uraltseva, "Linear and Quasilinear Equations of Parabolic Type" (transl. from Russian), AMS, Providence, RI, 1967.
[19] Z. Lewandowski and H. Beyenal, "Fundamentals of Biofilm Research," CRC Press, Boca Raton, 2007.
[20] R. E. Mickens, *Nonstandard finite difference schemes*, in Mickens RE (ed), "Applications of Nonstandard Finite Difference Schemes," World Scientific, Singapore, 2000.
[21] F. V. Passos, H. P. Fleming, D. F. Ollis, H. M. Hassan and R. M. Fekler, *Modeling the specific growth rate of Lactobacillus planarum in cucumber extract*, Appl. Microbiol. Biotechnol, **40** (1993), 143–150.
[22] Y. Saad, *SPARSKIT: a basic tool kit for sparse matrix computations*, http://www-users.cs.umn.edu/~saad/software/SPARSKIT/sparskit.html, 1994.
[23] P. S. Stewart, *Diffusion in biofilms*, J. Bacteriol., **185** (2003), 1485–1491.
[24] O. Wanner and W. Gujer, *A multispecies biofilm model*, Biotech. & Bioeng., **28** (1986), 314–328.
[25] O. Wanner, H. Eberl, E. Morgenroth, D. Noguera, C. Picioreanu, B. Rittmann and M. van Loosdrecht (IWA Task Group on Biofilm Modeling), "Mathematical Modeling of Biofilms," IWAPublishing, London, 2006.

Received September 2008; revised December 2008.

E-mail address: hkhasseh@uoguelph.ca
E-mail address: messoud.efendiyev@helmholtz-muenchen.de
E-mail address: heberl@uoguelph.ca